

Comparative analysis of nitric oxide synthase immunoreactivity in the sacral spinal cord of the cat, macaque and human

A. H. PULLEN¹, P. HUMPHREYS¹ AND R. G. BAXTER²

¹Sobell Department of Neurophysiology, Institute of Neurology, Queen Square, and ²Royal London Hospital Medical College, Whitechapel, London, UK

(Accepted 18 March 1997)

ABSTRACT

Nitric oxide synthase immunoreactivity (bNOS-ir) was examined in the sacral spinal cord of the cat, macaque monkey and human using an antibody to the c-terminal region of neuronal NOS. In S2 of all 3 species NOS-ir was identified in both dorsal and ventral horns. In cat, monkey and human, bNOS-ir occurred in sensory neurons of superficial laminae and the base of the dorsal horn, in autonomic neurons around the central canal and in the intermediolateral sacral spinal nucleus. In all 3 species, a large proportion of somatic motor nuclei in the ventromedial (VM), ventrolateral (VL) nuclei, and Onuf's nucleus (ON) showed high bNOS-ir, while others exhibited markedly lower immunoreactivity. Validatory experiments showed separate cellular localisation for bNOS, inducible NOS (iNOS), and endothelial NOS (eNOS) with only bNOS being localised to neuronal perikarya. Comparative morphometric analyses of the relative proportions and diameters of motor neurons in the VL, VM and ON exhibiting high and low levels of bNOS-ir revealed statistically significant differences in proportions in individual nuclei, and differences in size were generally not statistically significant. Finally, a comparison between cat sacral and thoracic spinal cord showed bNOS-ir in motor neurons of S2 was subject to less animal and rostrocaudal segment variation than in T10.

Key words: Sacral motor neurons; Onuf's nucleus; nitric oxide; NOS; anal and urethral sphincters.

INTRODUCTION

Onuf's nucleus of the human and its homologues in cat and macaque innervate the striated muscles of the external anal and external urethral sphincters via the pudendal nerve (Onufrowicz, 1890; Sato et al. 1978; Roppolo et al. 1985; Pullen, 1988). In cat and the human the motor neurons innervating the sphincters exhibit the ultrastructural presynaptic morphology of somatic α -motoneurons (Pullen, 1988; Pullen et al. 1992) but also possess autonomic-like attributes, for example anatomical linkage to the sacral intermediolateral preganglionic parasympathetic nucleus (Rexed, 1954), a strong peptidergic input (Schroder, 1984; Katagiri et al. 1986; Kawatani et al. 1986; Gibson et al. 1988; Tashiro et al. 1989), and a direct midbrain input from nuclei co-innervating visceral

pathways (Holstege & Tan, 1987). While the external anal and urethral sphincter muscles receive the usual somatic cholinergic innervation associated with striated muscle, the pudendal nerve in the human also contains noncholinergic, nonadrenergic (NANC) axons conveying the putative neurotransmitter nitric oxide (NO), which relaxes the sphincter muscles (Burleigh, 1983; Parlani et al. 1993). Our recent examination of sacral motor neurons in cat (Pullen & Humphreys, 1995) showed that a high proportion of motor neurons in Onuf's nucleus exhibit NADPH-diaphorase activity and a similar proportion are immunoreactive for the brain-derived isoform of nitric oxide synthase (bNOS). Whether motor neurons in Onuf's nucleus of the human and primate are similarly NOS-immunoreactive is unclear since available descriptions of bNOS reactivity in spinal cord generally

focus on nonsacral segments where typically, only occasional motor neurons are described to be NOS-immunoreactive (Dun et al. 1993; Terenghi et al. 1993). The first aim of this study is to delineate the distribution of bNOS immunoreactivity in the sacral segments of the macaque monkey and neurologically normal human, and to compare the distributions obtained with that found in cat sacral spinal cord.

Intracellular NOS has been assessed both indirectly using NADPH-diaphorase histochemistry (on the premise that in some CNS regions diaphorase co-localises with NOS and some forms of NOS have diaphorase activity; Hope et al. 1991; Vincent & Hope, 1992; Matsumoto et al. 1993), and directly using immunocytochemistry (Blottner & Baumgarten, 1992; Dun et al. 1993; Saito et al. 1994). However, our previous study demonstrated that in cat sacral motor nuclei about 40% of motor neurons fail to exhibit co-localisation of diaphorase and bNOS suggesting functional differences in their localisation. A common finding is that few somatic motor neurons in rat and the human express diaphorase or bNOS (Dun et al. 1993; Terenghi et al. 1993; Saito et al. 1994), suggesting that either our finding of high numbers of bNOS immunoreactive motor neurons in cat sacral cord (Pullen & Humphreys, 1995; Pullen et al. 1995) represents a segmental variation, or that immunocytochemistry detects additional isoforms of NOS, e.g. endothelial NOS (eNOS) or inducible NOS (iNOS). The distribution of iNOS and eNOS in cat sacral cord has not been reported. The second aim of the study is to compare the relative topographical distribution of bNOS, iNOS, and eNOS immunoreactivity at sacral level.

MATERIALS AND METHODS

Examination of cat and macaque spinal cord

Animals

Sacral spinal cords were obtained from 6 adult cats deeply anaesthetised with Ketamine HCl (35 mg/kg, administered i.m) and perfusion-fixed intracardially with 4% paraformaldehyde + 0.1% glutaraldehyde in 50 mM phosphate buffered saline (PBS), pH 7.3. Inclusion of this low concentration of glutaraldehyde enhanced the ability to cut thinner sections with the vibrotome without significantly reducing antigenicity or enzyme activity. Samples of sacral spinal cord from 2 adult macaques (*Macaca fascicularis*) freshly perfusion-fixed with a similar fixative were kindly provided by colleagues in the department.

General protocol

In cat and monkey, Onuf's nucleus resides in segments S1–S2 (Sato et al. 1978; Roppolo et al. 1985; Pullen, 1988). Segments S1–S3 were removed from each cord, cut into transverse 3 mm slices, and vibratome sectioned at 30–40 µm. Sections from both cat and monkey were immunostained using the same protocol.

NOS immunocytochemistry

Vibroslice sections spinal cord were rinsed in 20 mM PBS supplemented with 20 mM glycine (to block aldehyde groups from fixatives), 0.02% saponin (tissue solubiliser), and bovine serum albumin (BSA; 1% or 0.1%). Nonspecific antigen was blocked by preincubating sections for 45 min in the same buffer also containing normal goat serum (NGS) and fetal calf serum (FCS) at 5% final concentrations. NOS was detected using commercial polyclonal antibodies raised in rabbit. Polyclonal antibodies to a synthetic peptide from the C-terminal of rat cerebellar nitric oxide synthase (bNOS) were obtained from Eurodiagnostica, Sweden, cat. no. B220–1 (dilution 1:800), and Affiniti (cat. no. NC3000; NOSI or bNOS, dilution 1:800). Both antibodies were diluted in 20 mM PBS containing 0.02% saponin, 20 mM glycine, 1% BSA, 1% FCS and 1% NGS. Sections were incubated in primary antibody for 16 to 48 h at 4 °C. Optimal results occurred in both cases with an incubation time of about 40 h. *Negative controls* consisted of sections incubated without primary antibody or in media containing heat-inactivated antibody. Incubated sections were washed, incubated for 5 h (37 °C) in biotinylated antirabbit IgG (Amersham plc) diluted 1:200 with 20 mM PBS – 0.02% saponin – 1% BSA. Following further washes in PBS, sections were transferred to streptavidin-horseradish peroxidase (Amersham plc) diluted 1:300 in 20 mM PBS containing 0.02% saponin plus 0.1% BSA. Tissue bound HRP was detected with a PBS medium containing 1.3 mM 3–3 diaminobenzidine (DAB) substrate and 0.02% hydrogen peroxide.

Comparative distributions of bNOS, eNOS and iNOS

To compare the cytological distribution of immunoreactivity for bNOS, eNOS and iNOS in cat sacral spinal cord, individual groups of 5 sections of S2 were obtained from 2 further adult cats. In each animal the sections were nonserial but cut from the same 3 mm

transverse slice of cord. Although antibodies to bNOS from Eurodiagnostica and Affiniti gave identical results, Affiniti provided cognate peptides matching their antibodies. These experiments therefore only utilised antibody-peptide sets from Affiniti. *Group 1* was immunostained with the polyclonal Ab to bNOS (Affiniti no. NC3000, also known as NOS-I, dilution 1:800).

Group 2 was immunostained with anti bNOS (Affiniti, 1:800) that had been preincubated at 37 °C for 2 h with its complementary peptide (i.e. immunoadsorbed, cognate peptide Affiniti no. NP3100, 5 µg protein/ml diluted Ab). *Group 3* was immunostained with an antibody to eNOS alone (Affiniti no. N30030; also known as NOS-III, dilution 1:2500). *Group 4* was immunostained with anti eNOS following its immunoadsorption with its complementary peptide (5 µg protein/25 µl diluted Ab). *Group 5* was immunostained with antisera to iNOS alone (Affiniti no. N32030, also known as NOS-II, dilution 1:1000). *Group 6* was immunostained with anti-iNOS immunoadsorbed with its complementary peptide (5 µg protein/5 µl diluted Ab).

The immunogen used by Affiniti for the antibody to bNOS is a synthetic peptide equivalent to amino acid residues 1414–1429 of the rat NOS-I protein described by Bredt et al. (1991). The immunogen for the Affiniti antibody to iNOS is a 21 kDa protein fragment corresponding to amino acids 961–1144 of mouse iNOS, and for eNOS a 20.4 kDa protein fragment corresponding to amino acids 1030–1209 of human eNOS.

Subsequent qualitative examinations focused on the regional distribution of reactivity (i.e. whether it was confined to nerve fibres, nerve cells, glial cells), the relative intensity of staining (low, moderate, and intense), and position of reactivity (cytoplasmic, nuclear, perineuronal, neuropil). Regarding bNOS, a convenient internal control was provided by the sacral autonomic nuclei situated at the base of the dorsal horn and in the intermediolateral region (sacral parasympathetic nucleus, SPN; Nadelhaft et al. 1986). Neurons in these regions are characterised by their intense bNOS-immunoreactivity (Blottner & Baumgarten, 1992; Vizzard et al. 1993, 1994*a, b*).

Examination of human spinal cord

Archival specimens of sacral spinal cord obtained during routine autopsy were kindly provided by the neuropathology department of the Royal London Hospital. Formalin-fixed and paraffin embedded

cord from 4 subjects (41 y–93 y, postmortem delay 6 h–3 d) showing no neurological disease or sphincter dysfunction were sectioned at 10 µm and mounted on microscope slides. Sections were dewaxed, hydrated, and processed for the immunocytochemical detection of bNOS using the protocol described for cat tissue and, in initial trials, using identical antibody dilution and incubation times. Subsequent trials showed longer incubation times than those used for animal tissues were necessary to optimise differences in colour contrast between neurons and background neuropil and white matter (Pullen et al. 1995).

Quantitative analysis of level of immunostaining

The grey-scale levels of background neuropil and immunostained neurons were measured on digitised video images of each spinal cord histological section. For measurement, immunostained sections were standardised to 30 µm and photographed using 100ASA Kodak Estar film at final magnifications $\times 100$ or $\times 200$ and the illumination set to an equivalent colour temperature of 3700 °K. Photographic variation was minimised by photographing specimens from all monkey and human subjects at the same session, taking care that the microscope apertures and exposure time were constant throughout. Films were processed as a batch. This protocol is routinely used to examine the intensity of axonally transported label in the CNS following its cortical injection (Armond et al. 1997). The colour prints were digitally scanned into a PC and their video images converted to a 256-grey scale via Adobe-Photoshop software. Preliminary validity experiments showed that it was crucial that section thickness was standardised, and that scanner, software and PC VDU were gamma-corrected and calibrated against the same standard 256 grey-scale. This procedure follows that routinely used in microdensitometry (Joyce-Loebl; Image Analysis – Principles & Practice). Values were expressed as percentage absorbance (0% = white, 100% = black). The video images were analysed according to a strict procedure. Absorbance values were measured for 5 random regions of the neuropil and averaged to provide 'background' level of staining. Absorbance values were measured for each neuron in the photographic field. Inclusion criteria were that the neuron should display a nucleus and/or an obvious neuronal process, and its average absorbance could be calculated as the mean of at least 4 individual measurements made at random non overlapping sites in the cytoplasm.

RESULTS

Cytochemical controls

Omission of primary antibody (anti bNOS), heat-inactivated antibody, or biotinylated antirabbit IgG 'link' antibody all resulted in lack of staining in sections of cat, monkey and human spinal cord, strongly suggesting the observed immunoreactivity was due to binding between primary antibody and tissue-bound antigen.

Cat sacral spinal cord

To provide a baseline for examining primate and human spinal cords, a detailed examination of the cat sacral spinal cord was undertaken.

Nitric oxide synthase immunoreactivity (bNOS)

In cat sacral spinal cord bNOS immunoreactivity (bNOS-ir) occurred in the dorsal and ventral horns (Fig. 1*a*). In the dorsal horn, bNOS-ir occurred in neurons of laminae I and II, and in small bipolar neurons sited at the base of the dorsal horn in lamina VI (Fig. 1*b*). Small neurons adjacent to the central canal (Fig. 1*c*) and in the sacral parasympathetic nucleus (SPN; Fig. 1*d*) showed intense bNOS-ir. Interneurons in medial regions of the intermediate grey were generally nonreactive. In the ventral horn, motor neurons in Onuf's nucleus (ON), and the ventrolateral (VL) and ventromedial (VM) nuclei exhibited a spectrum of bNOS-ir which visually divided the motor neurons into 2 broad categories; those with higher and those with lower bNOS-ir. A larger proportion exhibited high bNOS-ir, than low or negligible bNOS-ir (Fig. 1*e, f*). In Onuf's nucleus both categories of motor neurons were identified in superior and inferior regions of the nucleus (Fig. 1*f*).

To provide a numerical index of the relative staining intensities in motor neurons, photographic images of immunostained vibratome sections were scanned into a computer, converted to a 256-point grey scale, and the mean absorbance values of individual motor neurons was measured and expressed as a percentage of random background 'staining' in the white and grey matter. In preliminary trials, motor neurons were first categorised by visual inspection, and the transition between high and low bNOS-ir was then determined quantitatively. Motor neurons classified visually as having 'high bNOS-ir' had absorbance values greater than 140% of background values (= 100%), while neurons with low or negligible NOS-ir

ranged between 100% and 130% of background. The transition between 'high' and 'low' NOS-ir corresponded to an absorbance value of approximately 140% of background.

Results of separate counts in the 3 sacral motor nuclei of motor neurons categorised by their high or low bNOS-ir are given in the Table (top section). In each case, *n* is the number of cats examined and the values given are the means of the pooled data from the 6 animals (\pm standard deviation). Paired Student's *t* tests showed that numerical differences between motor neurons with high and low bNOS were statistically significant ($P < 0.05$ – $P < 0.001$). Within individual nuclei, the relative diameters of motor neurons expressing high and low NOS-ir were similar (Table, lower section), and any differences were not statistically significant (paired Student's *t* test; $P > 0.1$). However, differences between the sizes of neurons of a given level of staining intensity between the 3 motor nuclei were statistically significant (paired Student's *t* test; $P < 0.001$).

Relative distributions of bNOS, eNOS and iNOS immunoreactivity

To verify that immunoreactivity seen in sacral motor neurons was not due to a combination of bNOS, eNOS (another constitutive isoform of NOS) and iNOS (inducible NOS), sections of sacral spinal cord from 2 additional cats were divided into 3 groups and immunostained for each of the 3 isoforms of NOS. In another 3 groups of sections, antigen-specificity of the antibodies was checked by immunoadsorption of each antibody with its complementary peptide before application to tissue. The chief differences between the distribution of bNOS-ir in cat sacral cords and the other 2 isoforms were that motor neurons in ON, VL and VM, and autonomic neurons in the SPN failed to exhibit either eNOS-ir or iNOS-ir. Reactivity to iNOS was extremely weak and restricted to regions around the central canal (presumed to be ependymal; Fig. 2*a*). By contrast, eNOS-ir was localised to small stellate cells both in the white and grey matter (presumed astrocytes; Fig. 2*d, e*). In the grey matter eNOS-ir occurred in stellate cells surrounding neurons and in fine processes in the neuropil (Fig. 2*d*). Reactivity was particularly prominent in laminae I, II and X. Both iNOS and eNOS-ir were completely abolished by preincubation of primary antibodies with their respective cognate peptides (illustrated for eNOS, Fig. 2*e, f*). bNOS-ir was abolished or severely compromised when anti-bNOS sera were immunoadsorbed with cognate peptides (Fig. 2*b, c*) but not

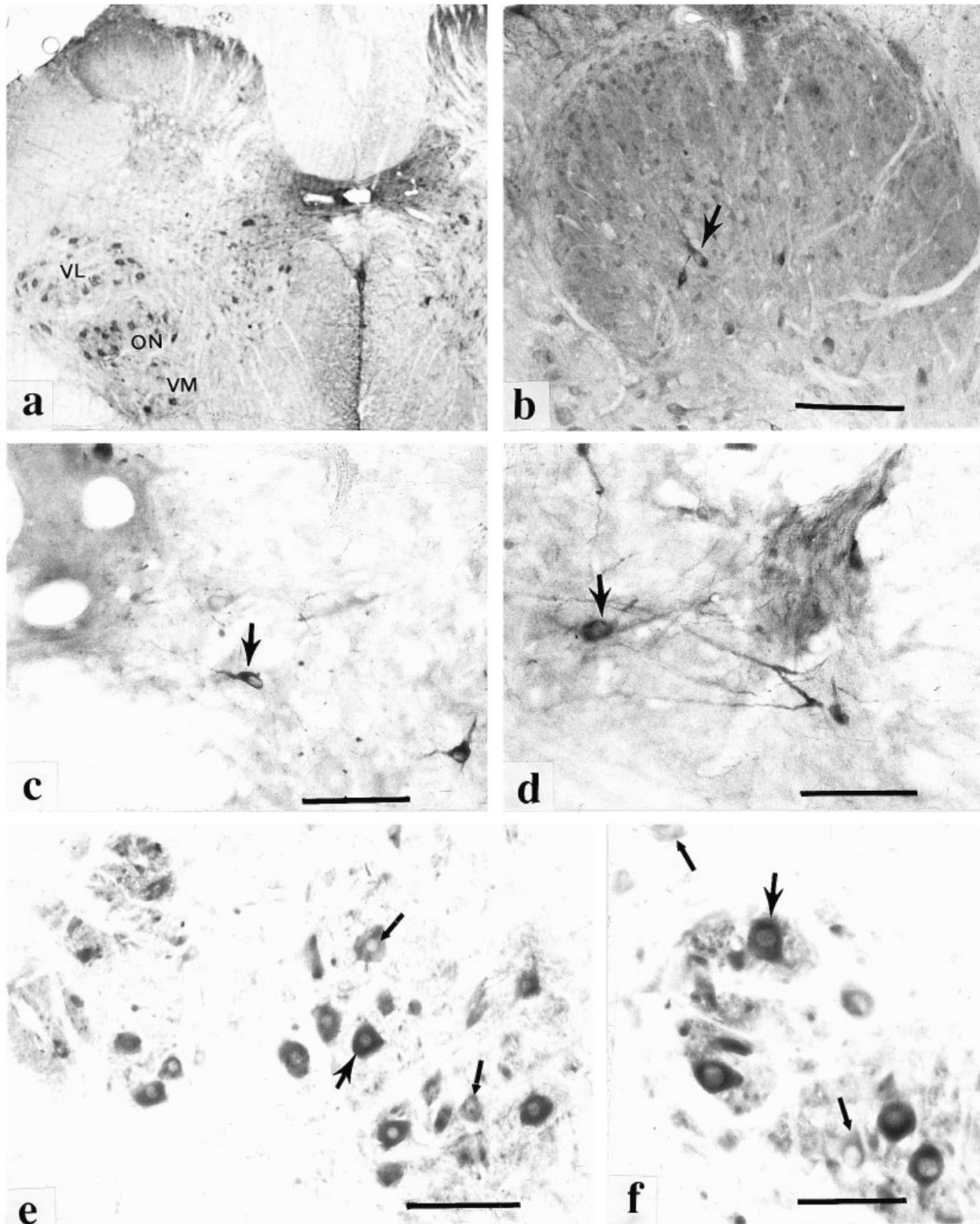


Fig. 1. Vibroslice sections of cat sacral spinal cord immunostained for brain-derived nitric oxide synthase (bNOS). bNOS-ir was identified (arrows) in (a) neurons of the ventrolateral (VL), ventromedial (VM) and Onuf's (ON) motor nuclei, (b) sensory neurons in the dorsal horn, (c) sympathetic neurons adjacent to the central canal and (d) in parasympathetic neurons of the intermediolateral nucleus. A large number of motor neurons in VL (e) and ON (f) exhibit bNOS-ir (large arrows), but some others have markedly lower immunoreactivity (small arrows in e and f). Bars, b, e: 50 μ m; c, d, f: 100 μ m.

Table. Comparison between relative proportions and sizes of motor neurons in Onuf's nucleus and the ventromedial and ventrolateral nuclei of the cat sacral spinal cord distinguished on the basis of their high or low level of immunostaining for bNOS.

	NOS [high]						NOS [low]						high vs low		
	n	Min	Max	Mean	S.D.	S.E.M.	n	Min	Max	Mean	S.D.	S.E.M.	t	D.F.	P
(a) Neuron proportions in cat based on number of experiments															
Onuf's nucleus	6	53.0	81.3	67.5	9.7	4.0	6	18.8	47.0	32.5	9.7	3.9	6.25	10	< 0.001
Ventrolateral nucleus	6	59.8	70.1	66.8	4.2	1.1	6	28.1	40.2	33.2	4.2	1.7	13.8	10	< 0.001
Ventromedial nucleus	5	45.8	64.2	55.6	6.9	3.1	5	35.8	54.2	44.4	6.9	1.3	2.57	8	< 0.05
(b) Neuron sizes in cat based on number of experiments															
Onuf's nucleus	6	12.25	62.15	29.09	3.04	1.24	6	10	65.19	28.25	4.05	1.65	0.41	10	> 0.1
Ventrolateral nucleus	6	17.32	77.14	49.59	3.74	1.52	6	19.36	77.14	46.86	5.51	2.25	1.00	10	> 0.1
Ventromedial nucleus	5	14.14	75	38.53	3.61	1.61	5	17.32	67.08	39.96	2.61	1.17	0.72	8	> 0.01

with inappropriate peptide (e.g. eNOS). To further characterise the nature of eNOS, the reputed activation and proliferation of astrocytes induced by spinal cord injury was examined in sample sections of thoracic spinal cord taken from cats which had received a unilateral spinal hemisection at T10 (material kindly provided by Dr P. Kirkwood, Sobell Dept). Two segments caudal to the lesion (T12) eNOS-ir was enhanced in the ventral horn ipsilateral to the lesion, particularly in association with reactive motor neurons (compare Fig. 2*f* and 2*g*). Prominent eNOS-ir occurred in the ipsilateral damaged white matter and neuropil of T12. Elevated ipsilateral eNOS-ir is consistent with an injury-induced activation and proliferation of astrocytes.

It was concluded that bNOS-ir was confined to perikarya of somatic motor neurons and autonomic neurons of the SPN, and that iNOS-ir and eNOS-ir did not contribute to the immunostaining of motor neurons in the major sacral somatic motor nuclei of the cat. It was further concluded that eNOS-ir was localised to astrocytes and provided an injury-response confined to astrocytes and not shared by neurons in injured spinal cord.

Distribution of bNOS-ir in macaque sacral spinal cord

Relative to cat spinal cord, qualitative examinations of bNOS-immunoreactivity in vibratome sections of perfusion-fixed primate sacral spinal cord (S1–S2) showed a number of general similarities (Fig. 3*a*). Firstly, immunoreactive neurons were present both in the superficial regions (Fig. 3*b*) and the base of the dorsal horn, and also adjacent to the central canal (Fig. 3*d*). Secondly, small intensely immunostained neurons occurred within the intermediolateral (IML) nucleus (Fig. 3*c*). Thirdly, large diameter immuno-

reactive motor neurons were located in the ventrolateral and ventro-medial nuclei, and Onuf's nucleus. Representative motor neurons in the VM and Onuf's nuclei exhibiting high and low levels of NOS immunostaining are shown in Figure 3*e* and *f*. Relative to sacral cord in the cat, NOS-immunoreactive motor neurons in the VL, VM and Onuf's nucleus of the macaque were visually more prominent (and numerous) and fewer neurons exhibited lower levels of immunostaining. Moreover, axons traversing mediolaterally through Onuf's nucleus were bNOS-immunoreactive, as were the profiles of transversely sectioned longitudinal dendrite bundles which characterise this nucleus.

To verify the qualitative impression that 2 populations of sacral motor neurons differing in levels of NOS-ir were present in the monkey, absorbance values for individual motor neurons in each of the 3 sacral motor nuclei were measured, the values pooled and then plotted as a frequency distribution. Illustrated in Figure 5*a*, the distribution suggested bimodality distinguishing 2 populations of motor neurons with maximum absorbance values of 130–140% of background (representing neurons with lower levels of bNOS-ir), and 160–165% of background (higher levels of bNOS-ir). Statistical analysis revealed an asymmetric bimodal distribution with overall mean absorbance value of $144.3\% \pm 13.9\%$, a median at 148% and modes at 131.8% and 165%.

The relative proportions of sacral motor neurons expressing higher levels of bNOS-ir in each of the 3 somatic motor nuclei were calculated from counts of immunostained motor neurons made directly on the sections. In Onuf's nucleus, 41.1% expressed high bNOS-ir in the first monkey, and 36.9% in the second. In the VL corresponding values were 56.9% and 51.8%, and in the VM they were 30.8% and 40.4%. The relative sizes of sacral motor neurons

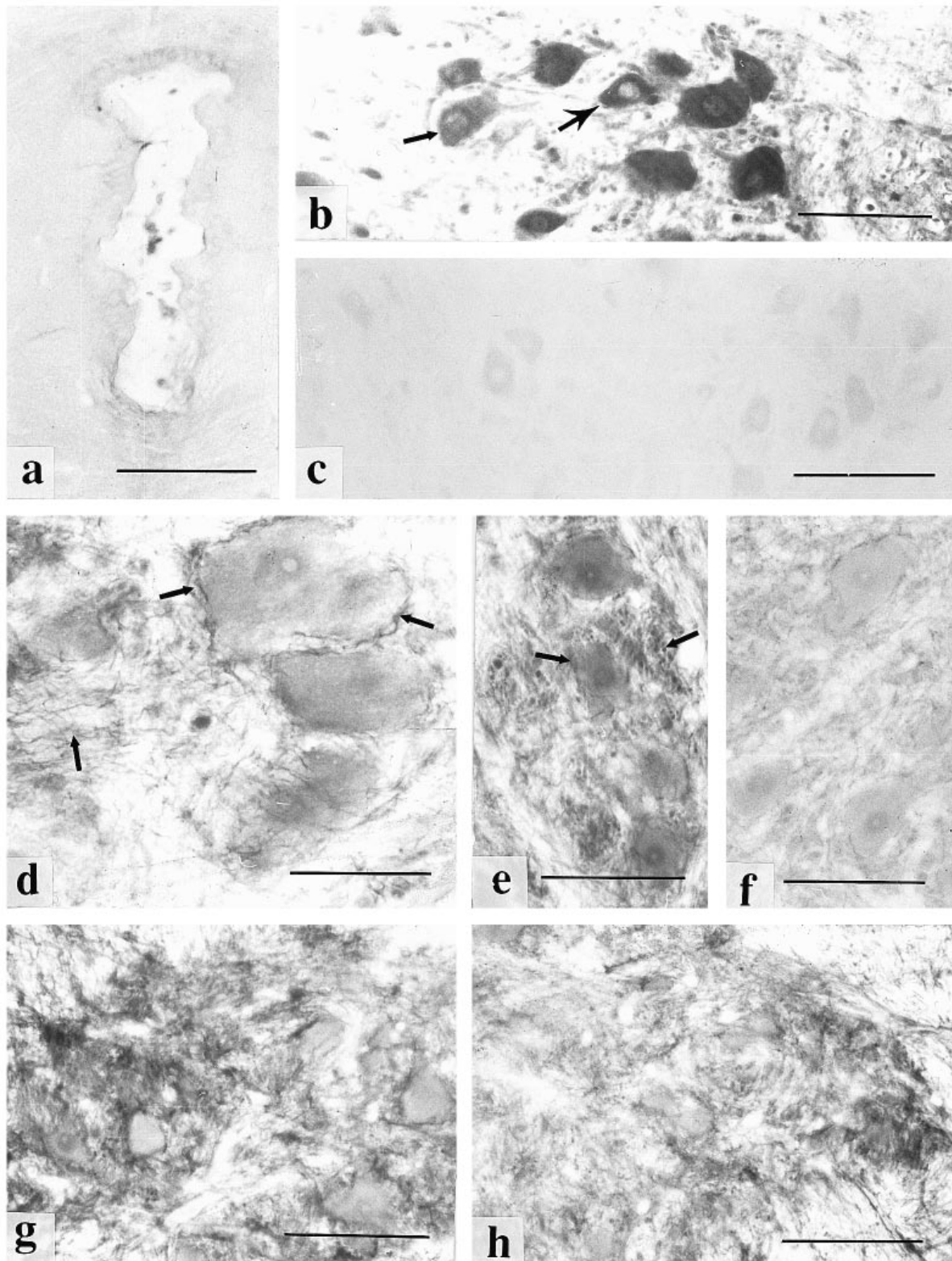


Fig. 2. Comparative cytological distributions of bNOS, eNOS and iNOS illustrated in vibratome sections of cat sacral spinal cord. (a) Low iNOS-ir in ependymal cells of the central canal; (b) bNOS-ir in sacral motor neurons; (c) markedly reduced bNOS-ir following preadsorption of antiserum with bNOS peptide; (d) eNOS-ir in fine processes (arrowed) investing motor neurons and in the neuropil of Onuf's nucleus (e); (f) reduced eNOS-ir following preadsorption of anti-eNOS with its cognate peptide; (g, h) eNOS-ir in the ventral horn of T12 2 wk following a spinal hemisection at T10; g is ipsilateral to the lesion, h is contralateral. Bars, a, d, 50 μ m; b, c, e-h, 100 μ m.

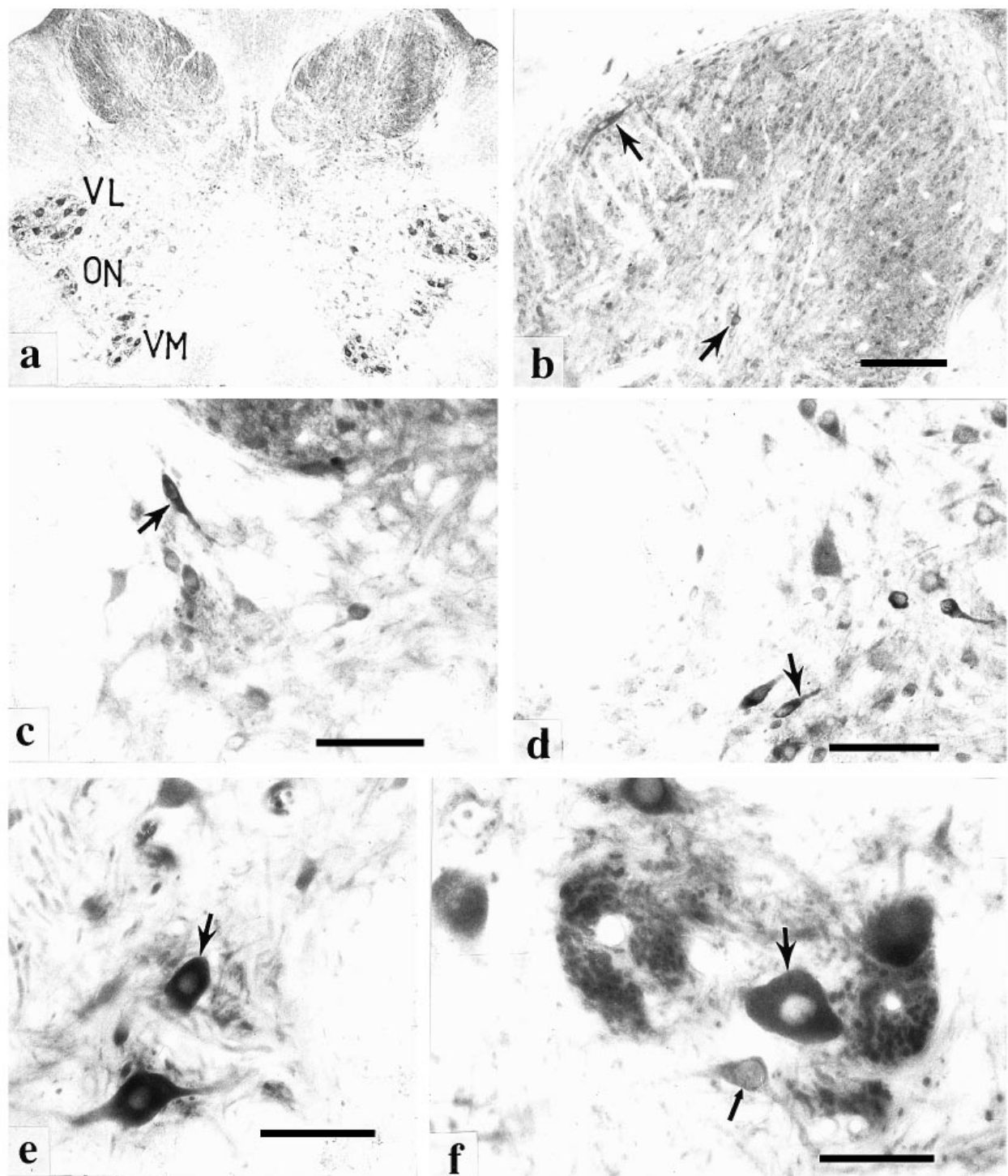


Fig. 3. Distribution of nitric oxide synthase immunoreactivity (bNOS-ir) in the sacral cord of *Macaca fascicularis*. In 50 µm vibroslice sections of S1, bNOS-ir occurred in neurons of (a) the ventrolateral (VL), ventromedial (VM) and Onuf's (ON) motor nuclei, (b) the dorsal horn (arrowed), (c) the parasympathetic intermediolateral nucleus, and (d) in small neurons adjacent to the central canal. In the ventral horn, many motor neurons in the VM (e) and ON (f) show intense bNOS-ir (large arrows), but others exhibit negligible bNOS-ir (e.g. small arrow in (f)). Bars, 50 µm.

expressing high and low bNOS-ir were determined by pooling data from the 2 monkeys. For Onuf's nucleus, the relative diameters of motor neurons with high and low bNOS-ir were $25.6 \mu\text{m} \pm 8.4 \mu\text{m}$ ($n = 112$) and $19.6 \mu\text{m} \pm 8.7 \mu\text{m}$ ($n = 173$) respect-

ively. A paired Students *t* test showed this difference to be significant ($t = 5.807$, D.F. = 283, $P < 0.001$). Corresponding diameters for the VL were $40.2 \mu\text{m} \pm 10.4 \mu\text{m}$ (high NOS-ir, $n = 348$) and $28.2 \mu\text{m} \pm 11.7 \mu\text{m}$ (low bNOS-ir, $n = 300$), and for

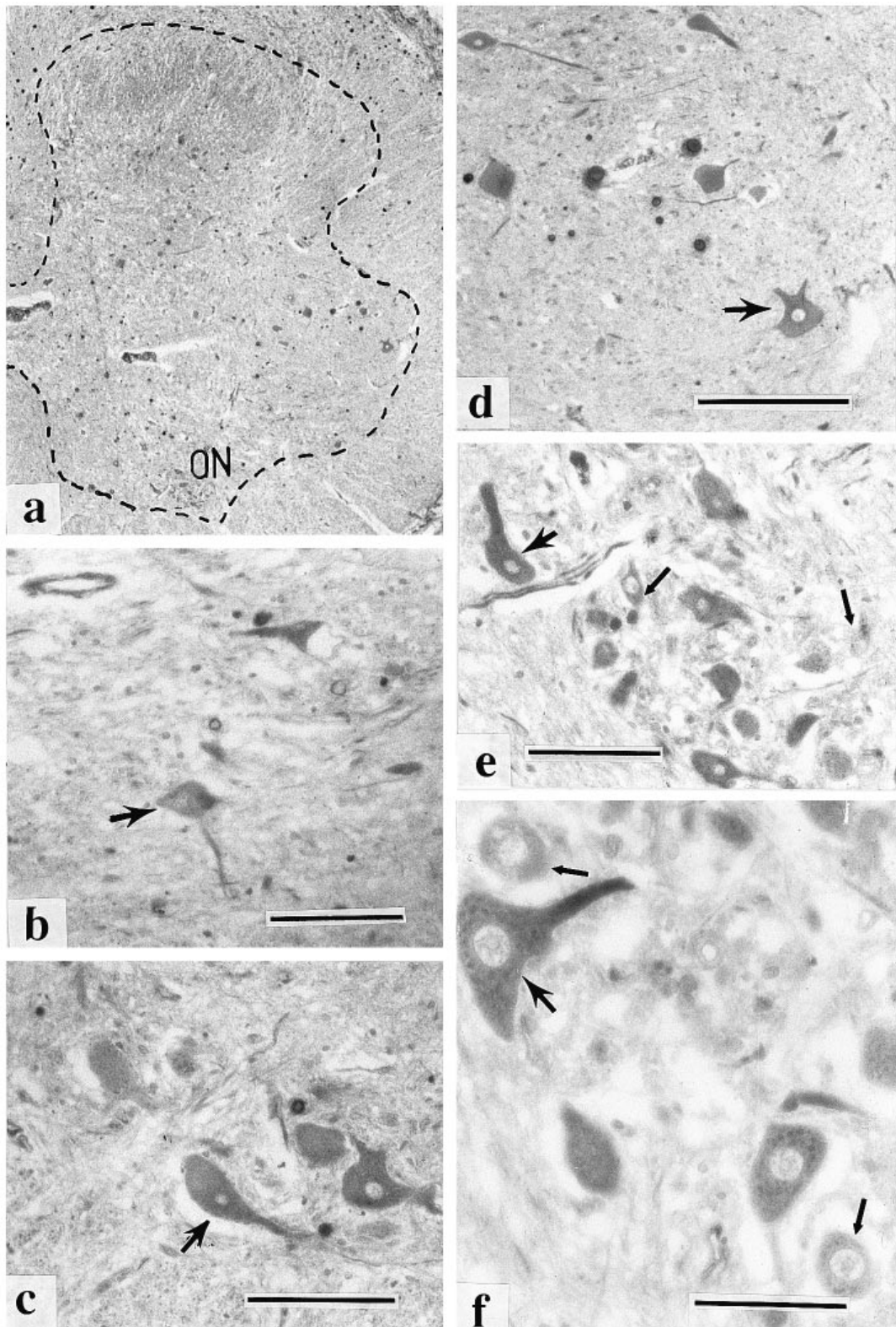


Fig. 4. Formaldehyde-fixed, wax-embedded sections of the human sacral spinal cord (S1) immunostained for bNOS. Typically, background staining is higher than in perfused animal tissue. bNOS-ir in (a) S1 (VL, VM and ON outlined), (b) neurons at the base of the dorsal horn and intermediolateral nucleus (arrowed), (c) motor neuron in the VM, (d) VL, and ON (e). As in monkey, some human sacral motor neurons have high levels of NOS-ir (larger arrows in e and f), while others have markedly lower NOS-ir (smaller arrows). Bars, b–e, 100 μ m; f, 50 μ m

the VM values were $31.2 \mu\text{m} \pm 11.4 \mu\text{m}$ (high bNOS, $n = 119$), and $18.8 \mu\text{m} \pm 7.5 \mu\text{m}$ (low bNOS-ir, $n = 200$). Differences between the sizes of neurons within the VL expressing high and low bNOS-ir were statistically significant ($t = 13.7$, D.F. 646, $P < 0.001$). Likewise the differences within the VM were also significant ($t = 9.925$, D.F. = 237, $P < 0.001$). Student's t tests also showed that the sizes of neurons expressing high bNOS were also statistically significant when compared between ON-VL, ON-VM, and VL-VM ($P < 0.001$ in each case).

Human sacral spinal cord

The immunocytochemical staining protocol applied to cat and monkey spinal cord required modification to optimise levels of neuronal bNOS-ir, relative to the background, because the combined effects of post mortem delay, prolonged immersion in formalin, and paraffin-wax embedding reduced antigenicity and raised levels of 'background' staining (Pullen et al. 1995). Optimal, immunostaining required short post-mortem delays (12 h), a longer incubation period (60–65 h, 4°C) and a short as possible period of immersion fixation. Post-mortem delays > 15 h precluded reliable immunostaining. Relative to perfusion-fixed material, immersion-fixed postmortem tissue generally demonstrated a higher level of background staining which was directly related to length of time tissue was stored in formalin. In general, the distribution of bNOS-immunoreactivity detected in S1–S2 was similar to that found in cat and the macaque, although the demarcation between white and grey matter was more difficult to discern (Fig. 4a). In particular, immunoreactivity occurred in neurons in the superficial dorsal horn and in small horizontally oriented neurons located between the central canal and extreme intermediolateral region of the grey matter (Fig. 4b). Immunoreactivity in the ventral horn was confined to motor neurons in the VM (Fig. 4c) and VL (Fig. 4d) nuclei and was especially prominent in Onuf's nucleus (Figs. 4e). Immunoreactivity was not uniform among motor neurons, some exhibited significantly lower levels of staining than others (e.g. motor neurons in Onuf's nucleus; Fig. 4f). Within some motor neurons reaction product was uniformly distributed within the cytosol, but in others it was displaced by accumulations of lipofuscin. Small neurons presumed to be interneurons located between these 3 major nuclei and the central canal in regions conforming to laminae VII–VIII exhibited negligible levels of immunoreactivity.

The qualitative impression that 2 populations of

sacral motor neurons differing in levels of bNOS-ir were also present in the neurologically normal human was also suggested by the nature of the frequency distribution constructed for the pooled measurements of absorbance values measured for individual motor neurons in each of the 3 sacral motor nuclei (Fig. 5b). Motor neurons with qualitatively lower levels of bNOS-ir had absorbance values between 125%–135% of background, and values for motor neurons expressing higher levels of NOS-ir ranged between 140%–155%. Overall, 67.4% of neurons in Onuf's nucleus expressed levels of bNOS $> 140\%$ of background ($32.8\% < 140\%$). Statistical analysis showed overall mean absorbance was $146.6\% \pm 17.8\%$, with the median at 141% and modes at 131% and 161%. Both modes are just within 1 s.d. of the mean, and true bimodality is therefore unproven. While some apparent qualitative differences occurred between the numbers of sacral motor neurons in the youngest (4th decade) and oldest (9th decade) subjects, the sample size for individual age-groups is too small to perform a statistically significant analysis. In a wider examination of the normal human sacral spinal cord (Tucker et al. 1994), the overall range of diameters of motor neurons measured in paraffin-wax embedded histological material of 6 subjects was found to be $7.7 \mu\text{m}$ – $60 \mu\text{m}$ (mean diameter, $26.62 \mu\text{m} \pm 2.66 \mu\text{m}$). In this immunocytochemical study, motor neurons in Onuf's nucleus possessing higher levels of bNOS-ir ranged between $19.4 \mu\text{m}$ and $44.7 \mu\text{m}$ in diameter (mean $29.3 \pm 6.8 \mu\text{m}$), while those in the VL ranged between $25 \mu\text{m}$ and $57 \mu\text{m}$ (mean $43.7 \mu\text{m} \pm 8.6 \mu\text{m}$), and those in the VM measured $27.4 \mu\text{m}$ – $52.9 \mu\text{m}$ (mean $38.1 \pm 6.5 \mu\text{m}$).

It was concluded that the general topographical distribution of bNOS in the sacral spinal cord of the monkey and human was very similar to that in the cat. Apart from slight species variation in relative numbers of neurons, the general finding was that at sacral level a large proportion of somatic sacral motor neurons exhibit bNOS-ir.

A common finding in the literature, however, is that in other segmental levels few motor neurons express NOS (Dun et al. 1993; Terenghi et al. 1993; Saito et al. 1994). The experiments reported above show that eNOS and iNOS do not contribute to the level of 'NOS' immunostaining in sacral motor neurons. It remained possible therefore that segmental differences might occur in bNOS expression. To examine whether sacral segments were different from other segments in this respect, a preliminary examination of bNOS-ir was undertaken in the thoracic cord of the cat where the well documented strong bNOS-ir of preganglionic

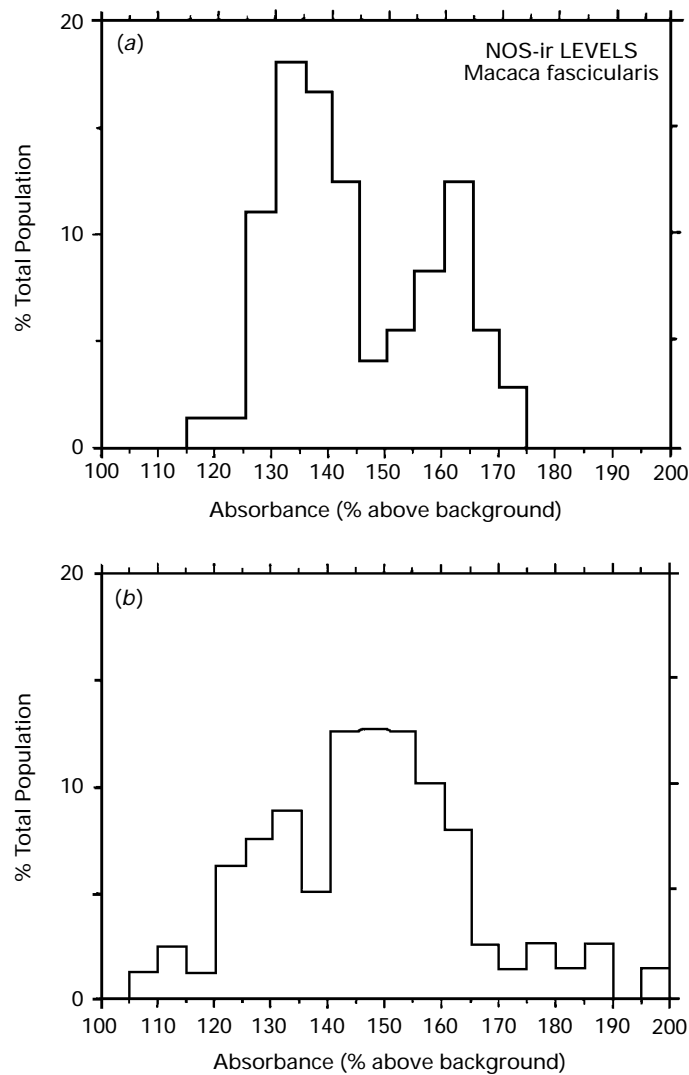


Fig. 5. Distribution profiles of microdensitometrically measured levels of bNOS-ir in individual pudendal motor neurons of (a) monkey, and (b) human. Staining level measured as an absorbance values on a 256-grey scale (0% = white, 100% = black) is expressed relative to 'background'. Distribution profiles both for monkey and human are bimodal, reflecting the 2 populations of motor neurons which qualitatively differ in bNOS-ir. Absorbance values around 130–140% above background correspond to motor neurons with low bNOS-ir and values 150–160% motor neurons with high NOS-ir.

parasympathetic neurons of the intermediolateral nucleus provides an intrinsic control for immunocytochemical method.

Distribution of bNOS-ir in thoracic segments of the cat

Thoracic autonomic and somatic motor neurons with unequivocal bNOS-ir were identified in each of the cats examined. Relative to thoracic somatic motor neurons, bNOS-ir was greater in small neurons in the dorsal horn (Fig 6a), in autonomic neurons of the intermediolateral nucleus (IML) (Fig. 6c) and in neurons and axons oriented horizontally between the central canal and IML (Fig. 6c). A common finding was that some sections of thoracic cord exhibited

distinct medial and lateral groups of motor neurons (up to 5 per group) with 50%–100% of them showing bNOS-ir. In other sections however, few motor neurons were found (~ 2–5 in toto) with perhaps 1 possessing bNOS-ir. This was in marked contrast to sacral cord where large numbers of bNOS-ir neurons occurred in every section. This observation is explained by retrograde labelling experiments which reveal that cat thoracic motor neurons innervating the external intercostal muscle are located along with levator costae motor neurons as a group in the ventrolateral tip of the ventral horn, whereas motor neurons projecting to the internal intercostal nerve are sited more dorsomedially (Fedorko, 1982; Johnson, 1986). Moreover, physiological experiments demonstrate a rostrocaudal reduction in numbers of

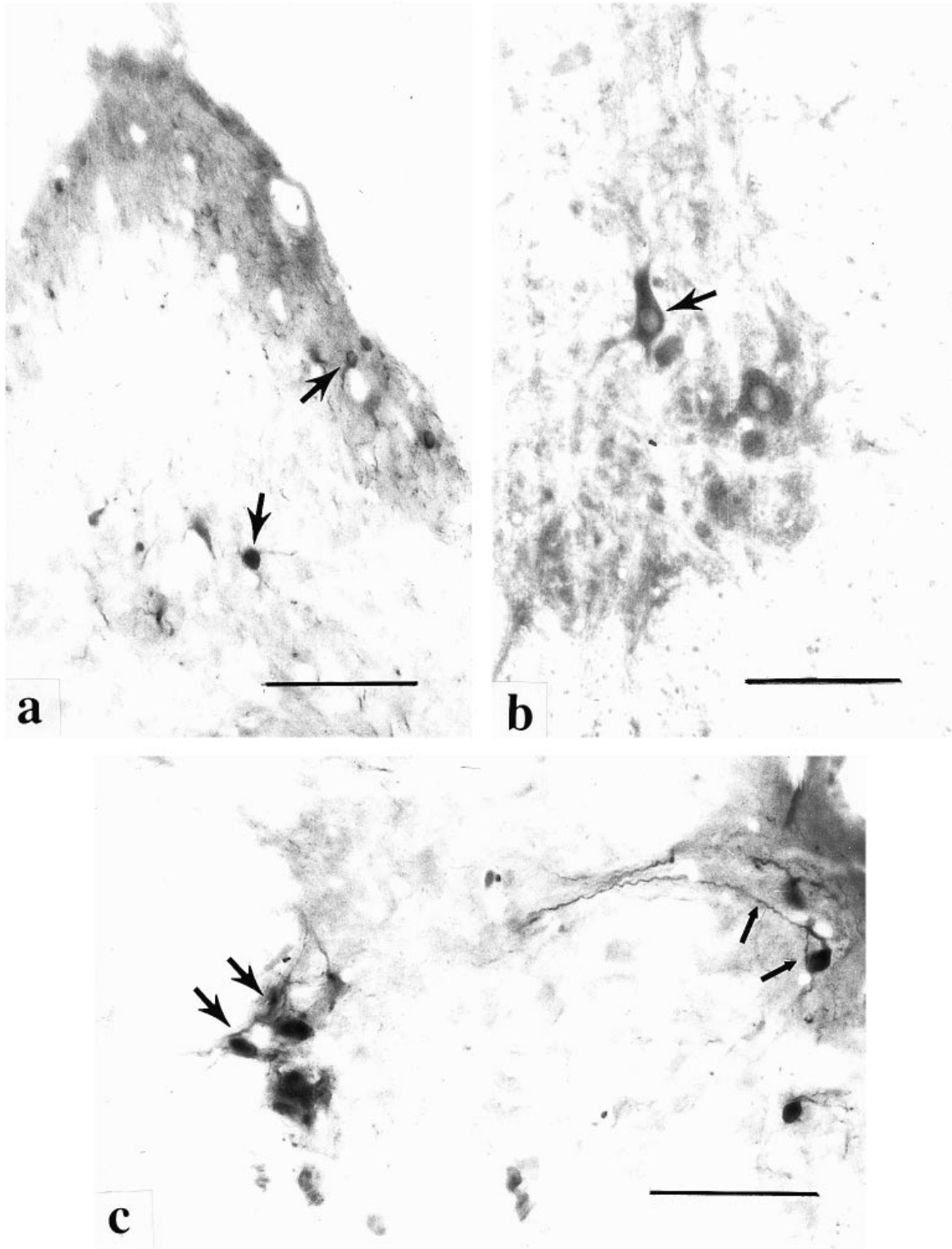


Fig. 6. bNOS-ir in 50 μ m vibratome sections of thoracic segment T12 of the cat, showing (arrowed) bNOS-ir in small neurons in superficial and deeper laminae of the dorsal horn (*a*), and in large motor neurons in the extreme ventrolateral ventral horn (*b*). In (*c*) 2 groups of bNOS-reactive neurons are shown; preganglionic parasympathetic neurons in the intermediolateral nucleus (IML, larger arrows) and small neurons adjacent to the central canal (smaller arrows) with fine immunoreactive processes which traverse the base of the dorsal horn towards the IML. Bars, *a*, *c*: 50 μ m; *b*, 100 μ m.

intercostal motor neurons within individual thoracic segments. Relative to the ventromedial region, bNOS-ir was more consistently present in motor neurons

located in extreme ventrolateral regions of the ventral horn (examples in Fig. 6*b*). It was concluded that somatic motor neurons in the cat thoracic spinal cord

exhibit bNOS-ir but, relative to sacral cord, the motor neurons exhibit a greater variability in both frequency and levels of immunostaining.

DISCUSSION

Results newly demonstrated that in cat a high proportion of sacral motor neurons immunostain for the brain-derived isoform of nitric oxide synthase (bNOS), while other sacral motor neurons show lower or no bNOS reactivity. Validatory experiments confirmed that iNOS and eNOS did not contribute to perikaryal immunostaining of NOS. Subsequent comparative qualitative examinations of bNOS-immunoreactivity in the sacral spinal cord of the macaque and human revealed their topographic distributions of bNOS to be identical, and strongly similar to that found in the cat. Finally, preliminary examinations of bNOS expression in other segments of cat spinal cord showed that sacral spinal cord possessed more bNOS-ir stained somatic motor neurons than thoracic segments, with less overall rostrocaudal and interanimal variability in numbers of immunoreactive motor neurons.

The clear demonstration of bNOS-ir in a majority of feline sacral somatic motor neurons is consistent with our previous preliminary findings (Pullen & Humphreys, 1995; Pullen et al. 1995). The identification of bNOS immunoreactivity in macaque and human *sacral* motor neurons has hitherto been unreported. Most previous studies of bNOS-immunoreactivity in cat and rat spinal cord focus on the sensory ganglia and sensory pathways in laminae I–IV, the thoracolumbar intermediolateral nuclei, and other preganglionic autonomic neurons (Terenghi et al. 1993; Saito et al. 1994). In rat, strong NOS-ir in varicosities apposed to motor neurons in the ventral horn have been described, but postsynaptic somata were found to be generally nonreactive (Saito et al. 1994). Previous studies of cat sacral spinal cord have focused specifically on NOS in visceral afferent/efferent pathways rather than in somatic motor nuclei (Vizzard et al. 1994b). The higher numbers of NOS-ir motor neurons found here in the macaque (40–50%), contrasts with the very low numbers of bNOS reactive motor neurons reported in the squirrel monkey by Dun et al. (1993). No previous reports describe the topography of NOS-ir in sacral spinal segments of the macaque or human. One issue raised by such marked differences in the reported occurrence of immunostained neurons is the possibility that observed perikaryal immunostaining represents a combination of different isoforms of NOS. Possible overlap

between bNOS, iNOS and eNOS is unlikely for three reasons. Firstly, eNOS and iNOS localised antigens in different cellular structures, which did not include sacral motor neurons. Secondly, antisera to bNOS, but not eNOS or iNOS immunostained autonomic neurons of the SPN which are known to contain bNOS (Blottner & Baumgarten, 1992; Vizzard et al. 1993, 1994b). Thirdly, an expected elevation of eNOS was produced in cat spinal cord following surgical injury. Injury is known to cause activation and proliferation of stellate-shaped astrocytes. However, motor neurons showed no corresponding reactivity for eNOS or iNOS. Moreover, the respective cytological reactivities for bNOS, eNOS and iNOS were abolished when antisera were immunoadsorbed with their respective complementary peptides, but staining for bNOS in motor neurons was not abolished by immunoadsorption with inappropriate peptides. It is therefore concluded that immunoreactivity in somatic motor neurons represents bNOS.

The exact functional significance of NOS in mammalian sacral motor neurons is uncertain. Neuronal NOS has been assigned a number of roles including intracellular messenger (stimulant of cGMP), and noncholinergic-nonadrenergic neurotransmitter in certain regions of the CNS, the myenteric plexus and sacral somatovisceral pathways (Snyder, 1992). In relation to the latter role, both the urinary bladder with its related urethral sphincters, and the colon with its internal and external anal sphincters are innervated by 3 major pathways. Firstly, somatic cholinergic efferents from motor neurons in Onuf's nucleus which innervate the external sphincters and are conveyed in the pudendal nerve; secondly, autonomic efferents (i.e. adrenergic and cholinergic) from the intermediolateral nucleus which project to the bladder, urethral junction, smooth muscle regions of the internal sphincters, and the colon via the hypogastric ganglion and pelvic nerve (Katagiri et al. 1986; Kawatani et al. 1986; Mawe et al. 1986, Nadelhaft et al. 1986; Thor et al. 1989); thirdly, in rat and the human, a nitric oxide dependent nonadrenergic, noncholinergic (NANC) efferent pathway conveyed by axons in the pudendal nerve which is responsible for sphincter relaxation (Burleigh, 1983; Parlani et al. 1993). The location of the parent motor neurons has not been reported, but the subpopulation of bNOS-immunoreactive motor neurons identified in ON in this study may be the parent motor neurons. By this logic, NOS-containing motor neurons in the VL and VM would enable relaxation of other perineal muscles. However, supporting physiological evidence is lacking. Alternatively, the possible significance of NO/NOS in sacral

motor nuclei may lie in its secondary messenger function.

In wider perspective, NOS has been implicated in biochemical pathways associated both with certain forms of excitotoxicity (Koh et al. 1986; Vincent & Hope, 1992) and in the abnormal regulation of intracellular free radicals preceding cell death (Vincent & Hope, 1992). In this context, the putative role of NOS in sacral motor neurons as second messenger activated by excessive excitatory activity, or as a protector, in response to intracellular accumulation of free radicals may be important. In the human, the sacral muscles and motor neurons exhibit a relative resistance to certain viral infections (e.g. polio; Kojima et al. 1989) and neurodegenerative diseases of somatic motor neurons (e.g. amyotrophic lateral sclerosis; Mannen et al. 1977), but not to some autonomic diseases (Sung et al. 1979). A better understanding of the relationship of NOS to neuronal phenotype may advance understanding of the ways different groups of segmental motor neurons respond to injury and neurodegenerative disease.

ACKNOWLEDGEMENTS

This project is supported by a project grant to AHP from The Wellcome Trust. We are indebted to Dr Joanne Martin (Royal London Hospital) and Prof. R. N. Lemon for provision of postmortem human and monkey material.

REFERENCES

- ARMOND J, OLIVIER E, EDGLEY SA, LEMON RN (1997) Postnatal development of corticospinal projections from motor cortex to the cervical enlargement in the macaque monkey. *Journal of Neuroscience* **17**, 251–266.
- BLOTTNER D, BAUMGARTEN H-G (1992) Nitric oxide synthetase (NOS)-containing sympathoadrenal cholinergic neurons of the rat IML-cell column: evidence from histochemistry, immunohistochemistry, and retrograde labeling. *Journal of Comparative Neurology* **316**, 45–55.
- BREDT DD, HWANG PM, GLATT CE, LOWENSTEIN C, REED RR, SNYDER SH (1991) Cloned and expressed nitric oxide synthase structurally resembles cytochrome P450. *Nature* **351**, 714–718.
- BURLEIGH DE (1983) Non-cholinergic, non-adrenergic inhibitory neurons in human internal anal sphincter muscle. *Journal of Pharmacology and Therapeutics* **35**, 258–260.
- DUN NJ, DUN SL, WU SY, FORSTERMANN U, SCHMIDT HH, TSENG LF (1993) Nitric oxide synthase immunoreactivity in the rat, mouse, cat and squirrel monkey spinal cord. *Neuroscience* **54**, 845–857.
- FEDORKO L (1982) Localisation of respiratory motoneurone pools in the cats' spinal cord. *Journal of Physiology* **332**, 28p.
- GIBSON SL, POLAK JM, KATAGIRI T, SU H, WELLER RO, BROWNELL DB et al. (1988) A comparison of the distribution of eight peptides in spinal cord from normal controls and cases of motor neuron disease with special reference to Onuf's nucleus. *Brain Research* **474**, 255–278.
- HOLSTEGE G, TAN J (1987) Supraspinal control of motoneurons innervating the striated muscles of the pelvic floor including urethral and anal sphincters in the cat. *Brain* **110**, 1323–1344.
- HOPE BT, MICHAEL GJ, KNIGGE KM, VINCENT SR (1991) Neuronal NADPH-diaphorase is a nitric oxide synthase. *Proceedings of the National Academy of Sciences of the USA* **88**, 2811–2814.
- JOHNSON IP (1986) A quantitative ultrastructural comparison of alpha and gamma motoneurons in the thoracic region of the spinal cord of the adult cat. *Journal of Anatomy*, **147**, 55–72.
- KATAGIRI T, GIBSON SJ, SU HC, POLAK JM (1986) Composition and central projections of the pudendal nerve in the rat investigated by combined peptide immunocytochemistry and retrograde fluorescent labelling. *Brain Research* **372**, 313–322.
- KAWATANI M, NAGEL J, DEGROAT WC (1986) Identification of neuropeptides in pelvic and pudendal afferent pathways to the sacral spinal cord of the cat. *Journal of Comparative Neurology* **249**, 117–132.
- KOH J-Y, PETERS S, CHOI DW (1986) Neurons containing NADPH-diaphorase are selectively resistant to quinolinate toxicity. *Science* **234**, 73–76.
- KOJIMA H, FURATA Y, FUJITA M, FUJIKOWA Y, NAGASHIMA K (1989) Onuf's motoneuron is resistant to poliovirus. *Journal of the Neurological Sciences* **93**, 85–92.
- MANNEN T, IWATA M, TOYOKURA M (1977) Preservation of a certain motoneurone group of the sacral cord in amyotrophic lateral sclerosis; its clinical significance. *Journal of Neurology, Neurosurgery and Psychiatry* **40**, 464–469.
- MATSUMOTO T, NAKANE M, POLLOCK JS, KUK JE, FORSTERMANN U (1993) A correlation between soluble brain nitric oxide synthase and NADPH-diaphorase activity is seen only after exposure of the tissue to fixative. *Neuroscience Letters* **155**, 61–64.
- MAWE GM, BRESNAHAN J, BEATTIE MS (1986) A light and electronmicroscope analysis of the sacral parasympathetic nucleus after labelling primary afferent and efferent elements with HRP. *Journal of Comparative Neurology* **250**, 33–57.
- NADELHAFT I, DEGROAT W, MORGAN C (1986) The distribution and morphology of parasympathetic preganglionic neurons in the cat spinal sacral spinal cord as revealed by horseradish peroxidase applied to sacral ventral roots. *Journal of Comparative Neurology* **249**, 48–56.
- ONUFROWICZ B (1890) On the arrangement and function of the cell groups of the sacral region of the spinal cord in man. *Archives of Neurology and Psychopathology* **3**, 387–412.
- PARLANI M, CONTE B, MANZINI S (1993) Nonadrenergic, noncholinergic inhibitory control of the rat external urethral sphincter: involvement of nitric oxide. *Journal of Pharmacology and Experimental Therapeutics* **265**, 713–719.
- PULLEN AH (1988) Quantitative synaptology of feline motoneurons to external anal sphincter muscle. *Journal of Comparative Neurology* **269**, 414–424.
- PULLEN AH, MARTIN JE, SWASH M (1992) Ultrastructure of presynaptic input to motor neurons in Onuf's nucleus: controls and motor neurone disease. *Neuropathology and Applied Neurobiology* **18**, 213–231.
- PULLEN AH, BAXTER RG, MARTIN JE (1995) Demonstration of nitric oxide synthetase in sacral motor neurons of the human and cat using antigen retrieval procedures. *Neuropathology and Applied Neurobiology* **21**, 455.
- PULLEN AH, HUMPHREYS P (1995) Diversity in localisation of nitric oxide synthase antigen and NADPH-diaphorase histochemical staining in sacral somatic motor neurones of the cat. *Neuroscience Letters* **196**, 33–36.
- REXED BA (1954) A cytoarchitectonic atlas of the spinal cord in the cat. *Journal of Comparative Neurology* **100**, 297–379.
- ROPPOLO JR, NADELHAFT I, DEGROAT WC (1985) The organisation of pudendal motoneurons and primary afferent projections in the spinal cord of the rhesus monkey revealed by horseradish peroxidase. *Journal of Comparative Neurology* **234**, 475–488.

- SAITO S, KIDD GJ, TRAPP BD, DAWSON TM, BREDT DS, WILSON DA et al. (1994) Rat spinal cord neurons contain nitric oxide synthase. *Neuroscience* **59**, 447–456.
- SATO M, MIZUNO N, KONISHI A (1978) Localisation of motoneurons innervating peroneal muscles: an HRP study in cat. *Brain Research* **140**, 149–154.
- SCHRODER HD (1984) Somatostatin in the caudal spinal cord: an immunohistochemical study of the spinal centers involved in the innervation of the pelvic organs. *Journal of Comparative Neurology* **223**, 400–414.
- SNYDER SH (1992) Nitric oxide and neurons. *Current Opinion in Neurology* **2**, 323–327.
- SUNG JH, MASTRI AE, SEGAL E (1979) Pathology of Shy-Drager syndrome. *Journal of Neuropathology and Experimental Neurology* **38**, 353–368.
- TASHIRO T, SADOTA T, MATSUSHIMA R, MIZUNO N (1989) Convergence of serotonin-, enkephalin- and substance P-like immunoreactive afferent fibers on single pudendal moto-neurons in Onuf's nucleus of the cat: a light microscope study combining the triple immunocytochemical staining technique with the retrograde HRP-tracing method. *Brain Research* **481**, 392–398.
- TERENGI G, RIVEROS-MORENO V, HUDSON LD, IBRAHIM NBN, POLAK, JM (1993) Immuno-histochemistry of nitric oxide synthase demonstrates immunoreactive neurons in spinal cord and dorsal root ganglia of man and rat. *Journal of the Neurological Sciences* **118**, 34–37.
- THOR KB, MORGAN C, NADELHAFT I, HOUSTON M, DEGROAT WC (1989) Organisation of afferent and efferent pathways in the pudendal nerve of the female cat. *Journal of Comparative Neurology* **288**, 263–279.
- TUCKER D, PULLEN AH, MARTIN JE (1994) A morphological and quantitative study of Onuf's nucleus in the human spinal cord. *Journal of Pathology* **172** (Suppl.), 145A.
- VINCENT S.R, HOPE BT (1992) Neurons that say NO. *Trends in Neurosciences* **15**, 108–113.
- VIZZARD A, ERDMAN SL, DEGROAT WC (1993) Localization of NADPH-diaphorase in pelvic afferent and efferent pathways of the rat. *Neuroscience Letters* **15**, 272–76.
- VIZZARD MA, ERDMAN SL, ERICKSON VL, STEWART RJ, ROPPOLO JR, DEGROAT WC (1994a) Localisation of NADPH-diaphorase in the lumbosacral spinal cord and dorsal root ganglia of the cat. *Journal of Comparative Neurology* **339**, 62–75.
- VIZZARD MA, ERDMAN SL, FORSTERMANN U, DEGROAT WC (1994b) Differential distribution of nitric oxide synthase in neural pathways to the urogenital organs (urethra, penis, urinary bladder) of the rat. *Brain Research* **646**, 279–291.